Al-Rafidain Journal of Engineering Sciences

Journal homepage https://rjes.iq/index.php/rjes

ISSN 3005-3153 (Online)

Implementing theoretical and experimental model of miniature (Wickless) heat pipe performance

Dhurgham Dheyaa Mahdi[1,*], Zeina A. Abdul Redha[2]

[1,2]University of Baghdad, College of Engineering, Energy Department, Baghdad, Iraq
[1]Email: dhurgham.mahdi2109m@coeng.uobaghdad.edu.iq
[2]Email: dr.zeina.a@coeng.uobaghdad.edu.iq

ARTICLE INFO

Article history:
Received 06 April 2024
Revised 08 April 2024,
Accepted 18 April 2024,
Available online 18 April 2024

Keywords:
Wickless heat pipes;
CFD simulation;
optimization methodology,
experimental work,
finned heat pipe;
cooling smart device,
inclination angle.

ABSTRACT

This paper shows an experimental and numerical analysis of heat transfer (h.t) for wickless heat pipe (h.p) and a performance (perf.) optimization methodology to enhancement h.t for h.p. Firstly the study focuses on the perf. miniature sample under inclination angles of (0°, 45° and 90°) experimentally for each power input (2.5 , 5 , 7.5) watt, starting with 2.5 watt, then for 5 watt , etc. Water as a working fluid (w.f) for all cases. Secondly we focuses on h.t experimental results of a cooler part were performed and validated using numerical simulation by ANSYS FLUENT. The objective of this paper is to conduct a comparative study on h.p perf. with different input powers subjected to different orientations. The inclination of an h.p very important for its perf. . The effect of h.p orientation on the perf. of the entire system is disorganized due to the much higher thermal resistance (th.r) on the air side of the cooler part .The results shows that the 45°orientation provides best thermal execution. The best behaviour of the h.p be at (2.5) W through steady average temperature (temp.) of condenser during (0 º, 45 º, 90 º) tilt angles. Idealism inclination angle for h.p is (45°), and the thermal perf. of the h.p is at this tilt angle. It observed from experimental readings and CFD simulation, the lowest pressure at lowest temp. Difference between heater and condenser sections. With thermal capacity increase, fluid pressure drop turn into maximum and difference in temp. between evaporator and condenser increases.

1. Introduction

The h.p is a passive highly effective device for h.t at high rates over considerable distances with small temp. drops, the construction is simple, exceptional flexibility and easy control without external power. A typical h.p is a closed duct filled by a liquid and its vapor.

A heat pipe consists of three sections, the heat addition section or evaporator, the heat rejection section or condenser and the isothermal (adiabatic section). These parts have an equal importance and can effect the heat pipe perf. [21] .

* Corresponding author E-mail address: dhurgham.mahdi2109m@coeng.uobaghdad.edu.iq
https://doi.org/10.61268/80svmj95

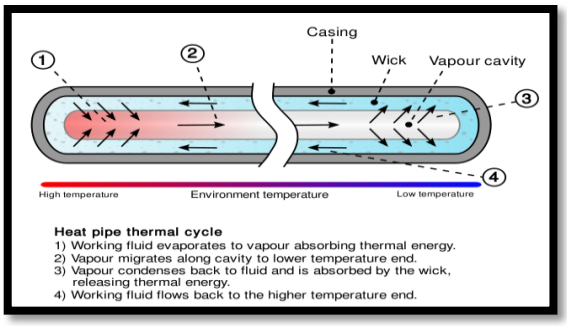

Figure (1) Heat pipe thermal cycle

At the high temp. interface of a h.p, a volatile liquid in touch with solid surface converted to vapour by absorbing heat from that surface. The vapour after travels along the h.p to the cold interface region and condensed into liquid, that releases latent heat. The liquid then returns to the heater area through either gravity or capillary action or centrifugal force and cycle repeats along it is works.

Heat pipes are highly effective thermal conductors, through the very high h.t coefficients for boiling and condensation (cond.) , The functional thermal conductivity changes h.p length, and can reach 100 kW/(m·K) for long h.p, in simile with approximately 0.4 kW/(m·K) for copper. As a result the H.P have:

- High thermal conductivity.
- Light weight and compact design.
- Uniform temperature.
- Autonomous and reliable with no maintenance required.

H.p consists of a locked pipe or tube made of a material that is harmonious with the working fluid like copper for water h.ps , aluminium for ammonia.

Usually, a vacuum is used to remove the air from empty pipe. Then h.p is partially filled with a working fluid (w.f) and then sealed. The w.f amount is chosen, the h.p contains both liquid and vapour over the operating temp. range.

It is very important to recommend operating temp. of a given h.p system. Below the operating temp., the liquid will be too cold and cannot be vaporized into a gas. Above the operating temp., liquid has turned to gas, and the circumferential temp. is too high for the gas to condensate. Through the walls of the h.p, thermal conduction (cond.) is still possible, but at a greatly reduced amount of thermal transition. A h.p consists mainly of two elements: the vacuum-sealed container (the working length of the device) and w.f. It may be used in many industrial fields to prevent and control temp. gradient such as ovens and furnace, System temp. control such as electronic equipment. Some applications require variable heat flow, so can fill that role like solar desalination system and circuit breaker. H.ps can be thought of as a technology capable of transferring self-contained heat a large amount of heat is transferred from the high temp. part to the low temp. one. Where high rate h.t in evap. and cond. occur in the device. Thermal energy is transferred in the form of heat depends on the phase change of the w.f with small temp. deference and large h.t combined with low thermal resistance (th.r) over the working length of the h.p . We aiming in this research paper mainly to h.t enhancement for wickless h.p by implementing experimentally and by simulation the optimum position (inclination) and input for designed miniature wickless h.p and choose water as w.f for all cases.

Zeina, A. Abdulredha [1] Designed and constructed of instrumented micro heat pipes for cooling electronic devices using smart technology and natural convection h.t. Experimental and theoretical studies were conducted in tilted closed conventional and annular micro heat pipes under different operating conditions to study heat flow, the influence of tilt angle, working fluid,

core type and tube shape affects the performance of heat pipes and the heat transfer process. Individual effects was examined by holding all parameters constant except the one being examined. To examine the effect of working two commonly used capillary Structures are selected to demonstrate the Effect of capillary structure on the heat transfer capacity of heat pipes. These are mesh wicks and powders interred wicks. This study also examined the impact of duct configuration (conventional, annular). The analyses are performed at different inclination angles, in order to see the effect of orientation on the heat pipe performance. And comparison between the novel configuration annular MHP and conventional MHP with this parameters. The steady state response of MHP (concentric annular and conventional) to various heat fluxes in evaporator and condenser regions are studied. The first analysis is done using annular MHP with water as working fluid. In this analysis, the effects of different properties of screen mesh wick structure and powder sintering wick have been studied. Same analyses were repeated for the acetone as w.f. For water and acetone h.p, results reveal that the mean temperature of the h.p increases for the same input power when using mesh type of wick structure in comparison with powder sintering wick.

The second analysiswas performedusinga conventional MHP withwater asthe working medium.Inthese analyses, the effects of the core structureof the screen fabricand various properties of the powder sinteredcorewere also examined. The same analysis was then repeated usingacetoneas theworking liquid. With the same input power and water and acetone heatpipes,it can be seen that there is a difference as the temperature increases using a mesh wick structure compared toa powder sinterewick structure. The study will also be conducted on water.When usinga traditional configuration and a screen as the wicking structure and a60° tilt angle, the micro heat pipe showed its maximum capacity at (188.4°C).

Acetone was also analyzed. When usinga ring structure and powder sinteringas the capillary s tructure and a30° tiltangle, the micro heat pipe provides maximum capacity at (190.92°C).

Based on these results, it is best to use a sieve for water.

Generally speaking, the best type of MHP is rings interred, which uses Acetone as the working fluid.

A theoretical analysis of the same experimental conditions was performed using Matlab equation control program.

The results are consistent with the current experimental results.

An experimental study was conducted by Manimaran et al. implement. [2] Studied the effects of input heat, charging filling rate and the slope of thermal characteristics of a (H.P), who less thermal resistance reportedly achieved at filling rate 75% and vertical direction.

Effect of tilt angle on heat productivity made from pulsating ammonia heat pipes and copper nano fluid heat the pipeline was described by Xue, Qu, and Senthilkurmar et al. implement. [3], [4] Or they indicate that thermal performance for number of heat pipes examined increases with increasing tilt angle.

Fadel et al. [5] developed a CFD model for simulation evaporation and condensation processes in TPCT. CFD Compare results with recoded data on temperature distribution and thermal resistance along heat pipes with different heat inputs. They reported that thermal properties improved whenever increasing heat input 172 watts with thermosiphon heat pipe performance. Many experimental studies had been performed to check the influence of working fluid and filling ratio and inclination angle on the performance of different heat pipes types, a lot of studies tested the perf. of two phase closed loop thermo-siphon (H.Ps) .

Noie [6] studied the evaporator aspect ratio and filling ratio impact (evap. length to evap. diameter) on perf. of heat transferring of the TPCT for heat input. It was concluded that

varying the filling ratio can reduces wall temp. of evap. depending on the prospect ratio.

Tang, Yongle, et al. [7] explain in their study, the thermal properties of ultra thin heat pipe (uthp) (thickness 1 mm) mesh cores with different mesh structures. The results show more meshes in the mesh core not only speed up but also reduce start up behaviour th.r for fixed operation. However, too high a mesh count also has disadvantages. this The corresponding permeability decreases with the increase of number of mesh , result in a large processing volume fluid flow resistance. The mesh building should be optimized for adequate capillary pumping capacity and good permeability to ensure the best perf. of UTHP. Number of needles From 120 in 1 to 220 in 1, 180 in 1 mesh should be a better choice for best results UTHP performance. In addition, via multi-directional tests, it was found that gravity acts an important factor in the thermal performance of UTHP. 200 in 1 Mesh Wicks numbers can help to get good anti-gravity the UTHP stability. Some main conclusions were obtained:

1. Increasing the number of stitches leads to an increase in run performance. Debugging time not only reduced, but improved achieve isothermal performance.
2. The mesh core with small number of mesh in UTHP shows poor effect heat dissipation perf., comprise high thermal resistance and evaporator temperatures. The number of grids increases, the heat increases UTHP's transfer performance is funded. Optimal mesh structure selection should be made get the best thermal perf. from UTHP.
3. In the range of 120 in 1 to 220 in 1 mesh, UTHP with 180-in-1 mesh wick for optimal thermal perf. . Neat mesh construction shouldn't just be a worry enough capillary force, large penetrability also.
4. The working inclination has obvious effect on heat generation transmission perf. of UTHP. With increasing slope angle, the maximum capacity of h.t and evaporator temp. of the UTHPs are notably improved.
5. The UTHPs with different mesh wick show many anti-gravity stability. Within the mesh no. range of 120 in_1 to 220 in_1, the UTHP with 200 in_1 mesh wick achieves the best possible anti-gravity operating.

Zhang, Hongzhe, et al , [8] Indicate that h.p are high h.t perf. device and high isothermal perf. for that widely used. Often most studies have focused on the average temp. characteristics for one or multiple heat pipes of the one type, lack of exhaustive analysis on the isothermal behaviour of many h.ps . Working principle of h.p structure tilt angle and fluid charge ratio affect thermal isothermal perf. . At this works and research on isothermal perf. application and influencing factors checked the heat pipes. Main conclusions are as follows:

1.The wick parameters have little effect on the isothermal perf. The arrangement of the h.p and the wick affects the flow of the steam working medium, which has The temp distribution has a greater influence. If gas flow is blocked smaller w.f , higher isothermal perf. of h.p**.**
2. Shape and length of different partitions of heat pipe has apparent effect on heat transfer and isotherm behaviour and condenser variations length has no appreciable effect on axial distribution of temp. or h.t conductivity at higher temp. . If the evaporator is too short, The working medium flow distance in the condenser is long, resulting in accumulation at the inlet of the condenser part of liquid w.f . The evaporator is too long, and the bottom of the evaporator section is prone to local overheating.
3. When the charge ratio is low, the evaporator is easy to overheat, and the number of starts is too high along the temp. difference in the h.p is large when charging high ratio. Only when the charging ratio is right, the h.p can start and working smoothly. The appropriate loading rate is 15-30% of the total internal volume.
4. The tilt angle will affect the isothermal perf. and take-off perf., especially in the condenser section. Along the vertical direction of gravity of the h.p decreases with the increase of the tilt angle, the effective heating area is increased. However, resistance of return is due to the reduction of the

component force, the cross section of the capacitor increases significantly heavy.
Heat pipes when tilted about 45, will be at best isothermal perf.
Maghrabie, Hussein M., et al [9] In his study outlines the numerical simulation Application of many heat pipes in various applications such as cooling, heating , solar power generation systems , nuclear reactors, , electric auto motives , waste heat recovery systems, low temperature etc. PHP can be used in cryogenic systems at extremely low temperatures. In addition to mechanism of heat transfer in PHP, The temperature at which working medium will boiling , plays a decisive role in thermal efficiency. So use a liquid with a very low boiling temperature effectively maintain the temp. of hydrogen, nitrogen, neon, etc.

Tharayil, Trijo, et al [10] Tested three h.ps (flattened with 400 mesh wick and flattened with 100 mesh wick and cylindrical with 100 mesh wick) , experiments were carried out on different he h.ps Inclined (+90o to -90o) with a heat load range of (10-60W). Preliminary tests show this suction mode of the fan provides more h.t than the blowing mode. The results show that the h.p inclination angle, , h.p section mesh size and heat inputs affect the thermal efficiency of heat pipes as they affect function liquid distribution on the evaporator part. Similarly, experimental results also explain that the 100-mesh wick (in flat and cylindrical h.ps) provide better h.t than 400 mesh wicks for all courts. Therefore it is recommended to use a wick of 100 mesh cylindrical and flat h.ps provide better perf., specifically in anti-gravity direction. The coefficient of h.t of evaporator varies in the range of 423-3876 W/m2K for all h.ps mentioned at various heat loads and inclinations. Similar to condenser heat transmission coefficients vary from 104 W/m2K to 1698 W/m2K. Flat h.p 100 mesh wick provides peak h.t for most tested conditions and heat loads. Since flat h.ps can be used inside flat electronic components, they preferred more than cylindrical h.ps for electronics cooling. In a 100-mesh heat pipe, evaporator temp. has a high reading on a positive slope and 400 mesh has a high reading the value of the anti-gravity direction. The top value of effective thermal conductivity for cylindrical h.p inclined at -45°, the observed power is 1416.5 W/m.K at 60 W. Anti gravity tests performed at different time intervals show that the h.p is trustable even when left idle for a period of time specific period. The h.p performance depends on filling ratio and tilt angle from horizon, M. L. Rahman, et al. [11].

Hu et al. [12] Evaluated experimentally that optimal performance at an inclination (θ = 40°), for wick and wickless h.ps.

Guo et al. [13] Explained that for sodium-potassium (Na-K) alloy h.p, inclination angle can affect the h.p perf.. It is noticed that increases in inclination angle from 0° to 50° also increases amount of h.t ; however, when θ exceeds 60°, h.t decreases gradually.
The purpose of this research is to examine cylindrical h.ps to provide the results required using h.ps in the best configuration, We presents an experimental and numerical heat transmission analysis of wick h.p and a perf. optimization methodology. The first section of the study focuses on the miniature sample perf. under different inclination angles of (0°,45° and 90°) and multi power input (2.5 , 5 , 7.5) Watt experimentally , these parameters used to evaluate the perf. of h.ps such best results from different directions in the absorption heat pipe.
In the second section of study, experimental results of the finned condenser heat pipe were performed and validated using numerical simulation by ANSYS FLUENT[19], [20].
From previous studies and our study, conclude that the best inclination angle is 45° and 5 W power input for wickless h.p miniature.

2. Experiments and Methods

In our research, we are strive to optimize wick h.p miniature , by changing geometry, to achieve best mechanical and thermal characteristics without changing dimensions, phase change material. We have modelled a cylindrical wickless h.p with an inner diameter of 11.55 mm, out diameter of 12

mm, 0.45 mm thickness, fin thickness 1 mm, fin outer diameter 25 mm, space between fins 1mm, number of fins 50.

Copper was used as the envelope material for its exceptional thermal conductivity, good mechanical properties and can resists corrosion, M.A. Chernysheva, et al. [14].

Thermal conductivity of copper is (387.6) W/m K, at constant pressure, specific heat capacity is (381) J/kg K and its density (8978) kg/m3. The h.p has been divided into (3) parts, (evaporator, adiabatic and condenser). The condenser lengths, adiabatic and the evaporator are 100 mm, 60 mm and 40 mm respectively.

We made a comparison between experimental work and numerical simulation by ANSYS FLUENT to validate the experimental work and inspect the perf. behaviour of miniature wickless h.p and heat dissipation amount through condenser zone and fins to free stream and analyze the results , at which inclination angle and power input will be the optimum perf. to the system.

In ANSYS FLUENT, available three different multiphase models in Euler - Eulerian Methods: (volume of fluid, mixture models, and Euler models). Works well in mixed models, the phases are treated as interference continuums, the mixed momentum equations are solved and velocities are assigned to describe the dispersed phase. Application of mixed models these include low particle loading flows, bubble flows, and cyclones, among others. Euler model is too complex multiphase option in ANSYS FLUENT, a series of pulses and solve the continuity equation for every phase. The phase exchange coefficient and pressure are introduced to attain coupling, and the coupling handle depends on involved stages type, Theory Guide (Release 15.0), in, ANSYS FLUENT [15]. Figures (2),(3), show the representation of the experimental setup. A 220 V A.C power source used and (power variac) for voltage variation. The h.p's length, outer diameter (200,12) mm respectively.

A voltmeter and ammeter are used to check input power and maintain accuracy. We used two pico log recording devices and laptop computer to monitor and record the readings (temp.) and (pressure) variability with respect to time. Before every reading, let the system works for time duration about 15 minutes, to get the steady-state condition. After that we started to fixing inclination angle (90°) and recording for each power input from (2.5 to 5 then 7.5) watt, later we change (45°) tilt and wait for 15 minutes also and repeat recording for same powers, at the end, same procedure for (0°) inclination angle had been performed.

Table (1) Wickless h.p specifications and dimensions.

HP material	Inner HP diameter (mm)	Outer HP diameter (mm)	Pipe thickness (mm)	Length of evap. section (mm)	Length of Cond. section (mm)	Working fluids
Copper	11.55	12	0.45	40	100	Water

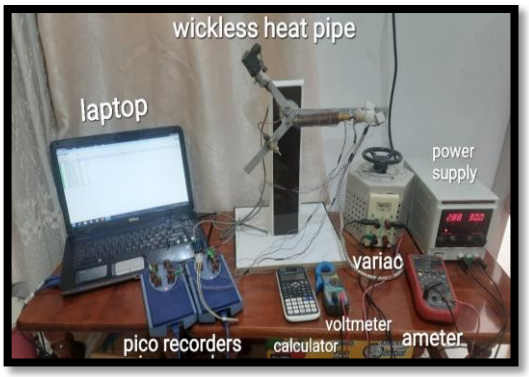

Figure (2) Experimental devices connection

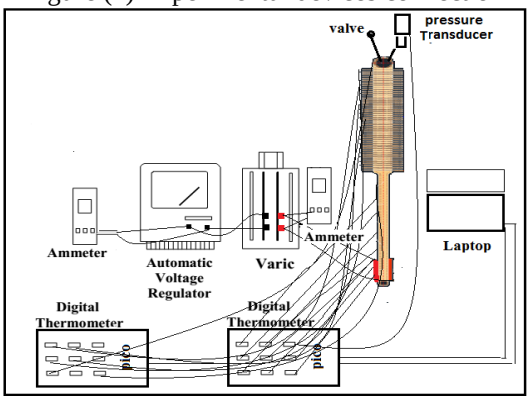

Figure (3) Schematic of Experimental h.p connection

Table (2) Thermocouples location for wickless heat pipe. miniature heat pipe.

Section	Thermocouple No.	Position mm
Evaporator	1	1
	2	10
	3	20
	4	30
Adiabatic	5	40
	6	60
	7	80
Condenser	8	100
	9	125
	10	150
	11	175
	12	199

The thermocouples (12) are attached in h.p surface to measure the temp. as in table (2) and other thermocouples end are attached with data recording system, connected to laptop.

3. CFD simulation

3.1 Model geometry and meshing

Design modular is used in ANSYS FLUENT to generate (design) three-dimension H.P geometry in a various directions. The geometry of the designed h.p are in Figures (4),(5) and table (1). Moreover, the final grid number elements was (350,305) and (226,681) nodes, it the best number for our sample as shown in figure (6), less that value, non uniform

distribution had been occur. If we choose mesh number more that value that will take a lot of time for each case running and no change in accuracy.

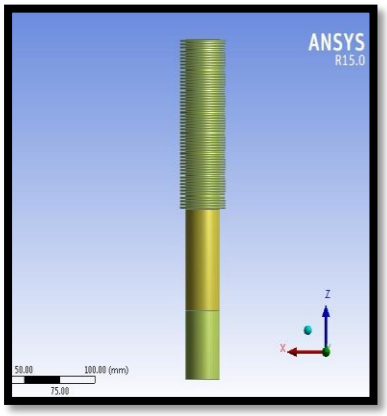

Figure (4) Design modular for wickless heat pipe sample in Ansys fluent.

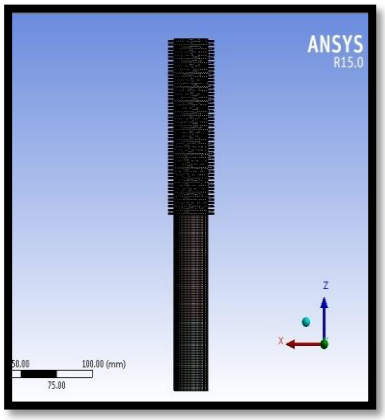

Figure (5) Mesh for wickless heat pipe sample in Ansys fluent.

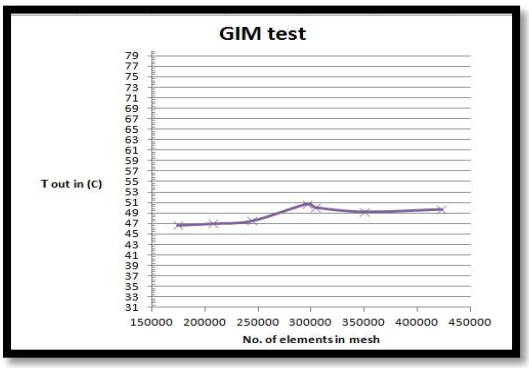

Figure (6) GIM test for wickless heat pipe sample in Ansys fluent.

3.2 CFD setup and solution procedure

3.2.1 Continuity equation:

In Volume of fluid (VOF) model, continuity equations for more than one phase volume fraction are solved to route the interfaces between the phases. For the vapour, the equation as follows:

$$\frac{\partial}{\partial t}(\alpha_v \rho_v) + \nabla.(\alpha_v \rho_v \vec{u}_v) = S_M \qquad (1)$$

where , $\alpha_v \rho_v \vec{u}_v$,are (volume fraction, density and velocity vector) of vapour phase, respectively.

S_M is transferred mass from liquid to vapour during evap. process and also opposite is true.

The primary phase volume fraction (air), could not be solved by above formula, and we can calculate by the following:

$$\sum_{l=1}^{n} \alpha_l = 1 \qquad (2)$$

The volume fraction equation is solved by explicit time formulation.

3.2.2 Momentum equation:

In the VOF model, the momentum equation, It is dependent on the volume fractions of all phases through average volume dynamic viscosity and average volume density, as the following term:

$$\frac{\partial}{\partial t}(\rho \vec{u}) + \nabla.(\rho \vec{u}\ \vec{u}) = -\nabla P + \nabla.[\mu(\nabla\vec{u} + \nabla\vec{u}^T) + \rho \vec{g} + \vec{F} \qquad (3)$$

$$\mu = \alpha_l \mu_l + \alpha_v \mu_v \qquad (4)$$

$$\rho = \alpha_l \rho_l + \alpha_v \rho_v \qquad (5)$$

where $\vec{g}$ is the gravity acceleration, $\vec{F}$ is the external force acting on the fluid, P is the pressure.

For including the surface tension effects for along the interface region between liquid and vapour, the continuum surface force(CSF) model , that was suggested by Brackbill et al. [16] and is applied to momentum equation:

$$F_{cs} = \sum_{pairs\ i\ j,<j} \sigma_{ij} \frac{\alpha_i \rho_i c_i \nabla \alpha_i + \alpha_i \rho_j c_i \nabla \alpha_j}{\frac{1}{2}(\rho_i + \rho_j)} \quad (6)$$

where C is the surface curvature between phase i and j, and σ_{ij} is the surface tension coefficient. For only liquid and vapour are in MCSHP:

$$c_l = -c_v \ and \ \nabla \alpha_l = -\nabla \alpha_{lv} \quad (7)$$

and Eq.(6) Could be simplified to:

$$F_{cs} = \sigma_{lv} \frac{\rho c_l \nabla \alpha_l}{\frac{1}{2}(\rho_l + \rho_v)} \quad (8)$$

which show that the surface tension is proportional to the average volume density.

3.2.3 Energy equation:-

In the VOF model, following term represent energy equation:

$$\frac{\partial(\rho E)}{\partial t} + \nabla.[\vec{u}(\rho E + \rho)] = \nabla.(k \nabla T) + s_E \quad (9)$$

Where s_E is the energy source term include contribution from evap. and cond., and averaged volume thermal conductivity (k) is given by relation below:

$$k = \alpha_l\, k_l + \alpha_v\, k_v \quad (10)$$

Both energy (E) and temp. (T) are treated as average mass variables as below:

$$E = \frac{a_l \rho_l E_l + a_v \rho_v E_v}{(a_l \rho_l + a_v \rho_v)} \quad (11)$$

where, E_l , E_v is the liquid phase energy and vapour phase energy, respectively.

$$Qc = h_c\, A_c\, (t_c - t_\infty) \quad (12)$$

Where: Q_c = heat flow through the convection heat flux in condenser.

A_c= surface area of the finned condenser (refer to equation):

$$Nu = \frac{h_c + h_c}{k} \quad (13)$$

$$Nu = (0.17)(Gr^* \Pr)^{\frac{1}{4}}$$

$$2 * 10^3 < Gr^* \Pr < 10^{16}$$

$$Q_w = cons. \quad (14)$$

$$h_c = \frac{k}{L_c}(0.17)(Gr^* \Pr)^{1/4} \quad (15)$$

h_c :The natural convection heat transfer coefficient.

$$Nu = \frac{g \beta q\, {L_c}^4}{K_a\, {v_a}^2} \quad (16)$$

$$Gr = \frac{g \beta (t_s - t_\infty)\, {L_c}^3}{{v_a}^2} \quad (17)$$

$$\beta = \frac{1}{(t_\infty + 273)} \quad ;\ t_\infty\ in\ c^\circ \quad (18)$$

$$\beta = \frac{1}{t(k^\circ)} \quad (19)$$

k_a= thermal conductivity of Air (mw/m.c°)·μ_a= dynamic viscosity for Air. ν_a= kinematics viscosity for Air. ρ_a= density for air. C_p= specific heat at constant pressure for air.

Pr= Prandtl number

$$Pr = \frac{\mu_a\, C_p}{k_a} \quad (20)$$

All properties are evaluated at film temperature

$$= \frac{t_c + t_{c\infty}}{2} \quad (21)$$

$$R = \frac{(t_e - t_c)}{{q_c}''} \quad (22)$$

$${q_c}'' = \frac{Q_c}{A_c} \quad (23)$$

q_c''=heat flux in condenser(kw/m^2), R = specific th.r

The heat flux due to conduction heat transfer to the vapour is:

$$q_{cond} = -k_v \frac{\partial T_v}{\partial n} \quad (24)$$

Where n is the direction normal of the interface.

To calculate the rejected heat by the condenser to the surroundings, we can write:

$$Q_c = A_c * h_c(t_c - t_\infty) + A_c * \sigma({t_c}^4 - {t_\infty}^4) \quad (25)$$

Where, Q_c= natural convection heat flow +radiation heat flow, σ=Stefan-Boltzmann constant = 5.669 * 10^{-8}w/m^2.k^2, subscript c refers to the condenser.

3.3 Set up and solution:

ANSYS FLUENT gives many separated algorithms for velocity and pressure. In CFD model, a combination of second-order and

(SIMPLE) algorithm for pressure-velocity coupling are used to increase accuracy through solving momentum equations and energy equations. Energy equation and K-epsilon (two-equation) viscous model with enhancing wall treatment was set. We selected thermal effects with curvature correction option. As well as, PRESTO and Geo - Reconstruct is used in simulations. In ANSYS FLUENT, We can use vof. model to show the phase-change flow and interfaces movement through the h.p. To simulate dynamic performance during the three phase flow, transient model was selected with time step size (1) sec., and time steps number was (900). The maximum iterations number was set as 20. The VOF model is designed for two or more immiscible fluids; the position of the interface between the fluids is useful, such as free-surface flows, stratified flows, large bubbles motion in a liquid, and the transient or steady tracking of any (gas – liquid) interface.

The flow inside h.p was regarded as transient, incompressible, laminar flow. Primary phase is air compared and a secondary phase for a liquid and other secondary phase as a vapour. The evap. and cond. processes latent heat of w.f boiling temp.s were defined in the UDF code to calculate the h.t and mass during the work. The (saturation) temp. of the w.f of is 373 K, it was specified to maintain that the process of (boiling/evaporating) starts once solution runs, all that to minimize the (convergence/solution) time, User's Guide ANSYS Fluent (Release 15.0), Modeling Multiphase Flows [17].

At the condenser part, the wall and w.f temp.s (condenser cooling temp.) are related to the convection across condenser surface and fins, environment temp. 303 k , the same of experimental circumstances. Moreover, w.f filling ratio of the h.p 70%, with inclination angles of (0◦, 45◦, 90◦),. The tilt angles are specified from the horizontal axis.

The surface tension force value from below correlation, J. Huang et al. [18].

$$\sigma = 0.09805856 - 1.845 \times 10^{-5}T - 2.3 \times 10^{-7}T^2 \quad (26)$$

The operating pressure is (400,000) Pa, coefficient of surface tension is (0.072), for the phase interaction. Phase change material speed (0.01 m/s) along the direction of h.p . Model selected was (multiphase) to simulate the phase change operation.

The initial temperature as 298 k, and firstly liquid volume fraction was fixed depend on the different rates. At initial condition is set was no heating. Moreover, (no-slip) boundary condition was fixed as at the inner wall of the h.p. To make simulation for heat added, constant heat flux is forced along external wall of evaporator during the process. The ends of the h.p was insulated, assumed there is no cooling or heating.

Brackbill et al. [16] studied surface tension force between the liquid and vapour phases in terms of the interfacial force, it was by activating CSF in ANSYS FLUENT [19],[20]. The applied CSF model was based on the proposed model**.**

We assumed in ANSYS FLUENT the w.f is only water, and copper metal specification used as listed in program options only. The limitation in our work is how perfume w.f percentage in case of (45°, 0°) inclination to maintain gravity effect on the fluid nature, that is done manually by design modular.

4. Results and discussion

4.1 Results of experiments

To perfume the experiment, tested wickless h.p miniature is used, in which heat input, pressure and surface temp. are the parameters to evaluate the perf. . The h.p works against the gravity also. The experiments are performed for three different tilt angles (θ) as (0°, 45°,and 90°) with power input (Qin) starting from (2.5 W to 7.5 W) with an increment of (2.5 W). Before every reading, let the system work for time duration about τ = 15 min, to get the steady-state condition. A pico log recording devices has been used to monitor the pressure and temp. variability with respect to time. The optimal results have been procured at (θ = 45°) inclination angle. The graph in Figure (7) shows the variation in average condenser temp. with respect to heat flux input by the heater. We can observe that for fixed w.f , the

variation in tilt angle has a major effect on the thermal perf. of h.p. Figure (8) shows the variability in evaporator temp. with respect to heat flux for a given powers and also the optimum behaviour at θ = 45°. Figure (9) illustrates the variability in average evaporator temp. with respect to inclination angle for a given powers, we can notice that the value of evaporator temperature at 90° different of behaviour of other inclinations and also condenser temp. would be higher , that means a part of the heater touch air in side h.p when it be in horizon position. That's lead to lower temp. deference at θ = 0°. And gravity forces increased due to the axial component, promote w.f transport from condenser to the evaporator region after 45º angle, Figure (10) explain the change in average condenser temp. with respect to inclination angle for three given powers. The changing in tilt angle in both experimental and simulation clearly effect the h.t of system, water and vapour particles transportation that affected by gravity force and circulation from (heater to condenser and return to heater) parts, the speed of carry heat is different also from one position to another. The thermal improvement has been happen in case of reducing cond. temp. to be close to environment, percentage of heat drop in h.p regarded accepted as natural cooling device, increasing surface area of cond. region and fin contribute to maintain requirements, also thermal conductivity amount and heat capacity of w.f (water represent had good capacity of heat). We can observe that the plot for (2.5 and 7.5) W has been the same to some extent, but for 5 W increased gradually duo tilt angle increasing. Average condenser temperature at θ = 45° be enclosed to other values of powers input. That enhance h.p works at good perf. and high efficiency at this tilt angle.

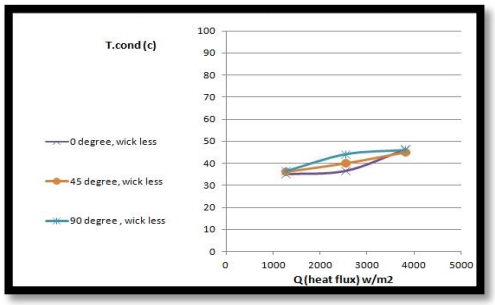

Figure (7) Condensation temperature with thermal heat flux for wickless heat pipe , Experimental readings

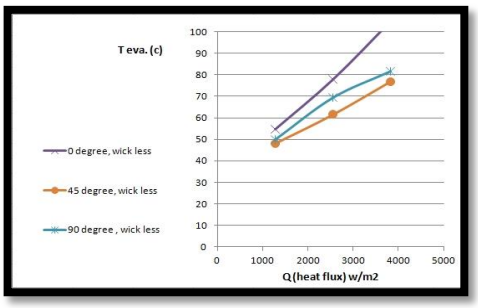

Figure (8) Evaporation temperature with thermal heat flux for wickless heat pipe Experimental readings

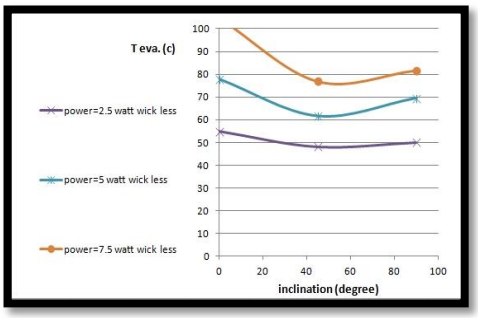

Figure (9) Evaporation temperature with inclination angle for wickless heat pipe , Experimental readings.

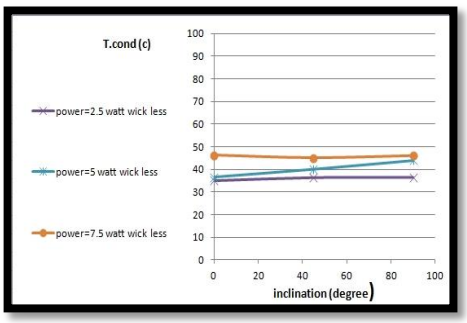

Figure (10) Condensation temperature with inclination angle for wickless heat pipe , Experimental readings.

4.2 Results of simulations

By contrasting between numerical simulation and measured temperatures, an experimental validation was perfumed with numerical simulations results. Figures (11) (12) (13) (14) (15) (16) (17) (18) (19) explains the temp. distribution across surface area of miniature wickless heat pipe for all inclination angles and powers. We can be observe that the temp. decreases toward condenser zone, while the maximum at heater zone. It is a uniform temp. distribution for (θ =

0°, 90°), whilst non uniform distribution at the beginning of condenser zone and at (water – air) interface region. The cause belong to w.f flow from condenser portion to evaporator part is improved by the enhanced gravity forces caused by the axial component, and following 45º tilt angle, the heat supplied is insufficient to make a difference. As a result, there are a decrease in radial heat transmission and an increase in th.r .

The Figure (20) shows the changing in average condenser temp. with respect to heat flux input by the heater. Figure (21) illustrates the variability in average condenser temp. with respect to inclination angle for three given powers. Figure (22) explain the variability in evaporator temp. with respect to inclination angle for a given powers .Figure (23) shows the variability in evaporator temp. with respect to heat flux for a given powers. The validation of experimental results with numerical simulation values illustrates that correct procedures and good efficiency of experimental devices, acceptable wickless heat pipe sample. The error percentage between numerical simulation and experimental results for condenser temp. varies from (2.13% to 8.2%) as shown in Table (5), this is regarded acceptable percentage of error.

Table (3) Percentage of error between experimental and Ansys for average conds. temperature.

No	Heat pipe type	Power (w)	Inclination (degree)	Error percentage of average T(cond.)
1	Wickless	7.5	90 º	6.6 %
2	Wickless	7.5	45 º	6.5 %
3	Wickless	7.5	0 º	8 %
4	Wickless	5	90 º	2.78 %
5	Wickless	5	45 º	8.2 %
6	Wickless	5	0 º	3.5 %
7	Wickless	2.5	90 º	2.75 %
8	Wickless	2.5	45 º	3.48 %
9	Wickless	2.5	0 º	2.13 %

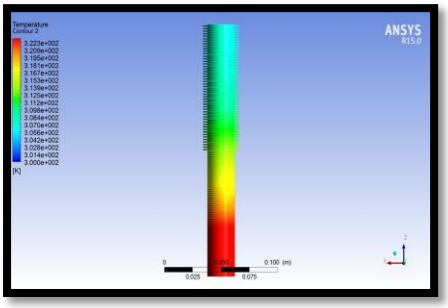

Figure (11) Temperature distribution in Ansys for wickless heat pipe , 2.5 watt input , 90 degree inclined.

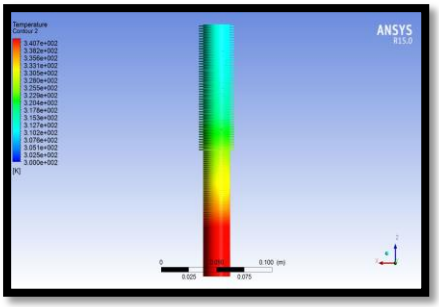

Figure (12) Temperature distribution in Ansys for wickless heat pipe , 5 watt input , 90 degree inclined.

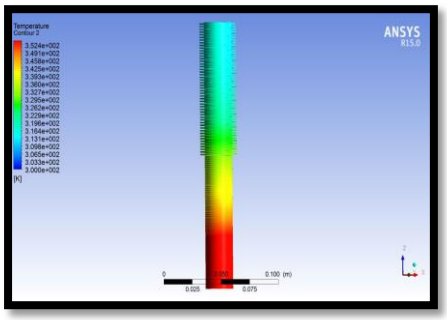

Figure (13) Temperature distribution in Ansys for wickless heat pipe , 7.5 watt input , 90 degree inclined.

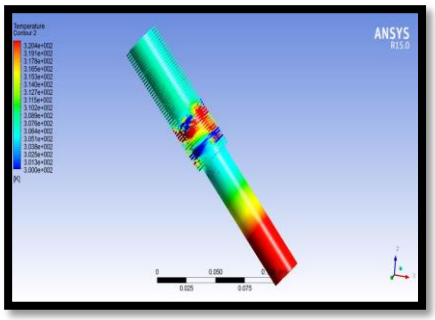

Figure (14) Temperature distribution in Ansys for wickless heat pipe , 2.5 watt input 45 degree inclined.

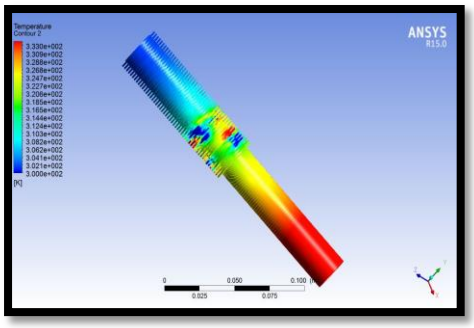

Figure (15) Temperature distribution in Ansys for wickless heat pipe ,5 watt input , 45 degree inclined.

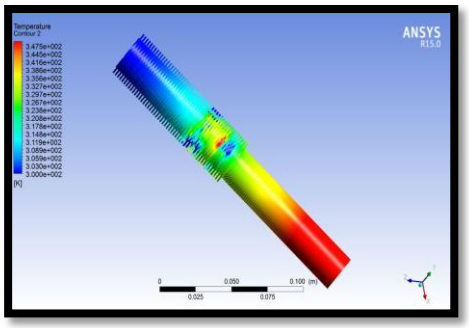

Figure (16) Temperature distribution in Ansys for wickless heat pipe , 7.5 watt input 45 degree inclined.

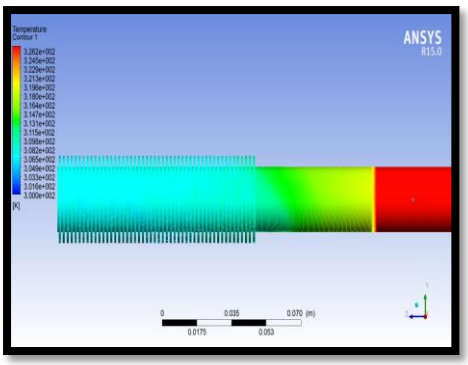

Figure (17) Temperature distribution in Ansys for wickless heat pipe , 2.5 watt input , 0 degree inclined.

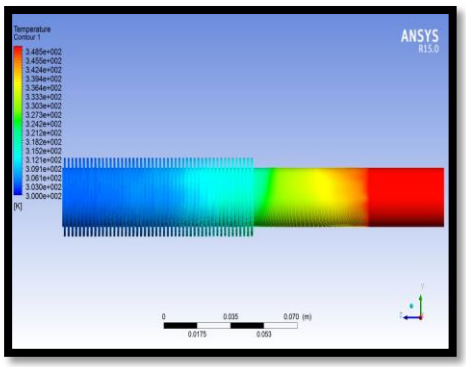

Figure (18) Temperature distribution in Ansys for wickless heat pipe , 5 watt input , , 0 degree inclined.

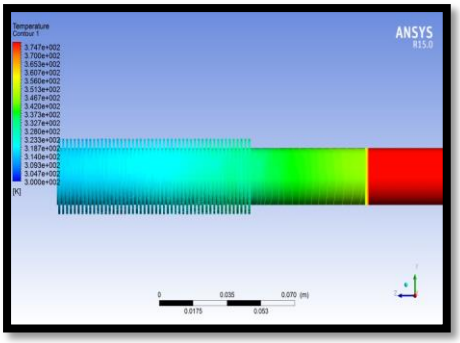

Figure (19) Temperature distribution in Ansys for wickless heat pipe ,7.5 watt input , 0 degree inclined.

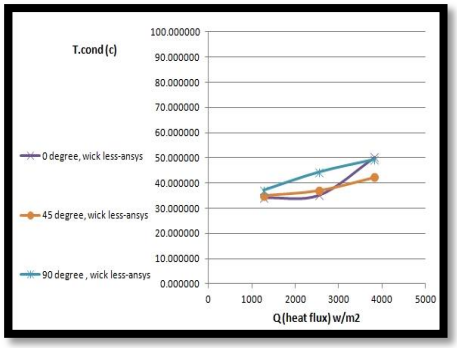

Figure (20) Condensation temperature with thermal heat flux for wickless heat pipe Ansys readings.

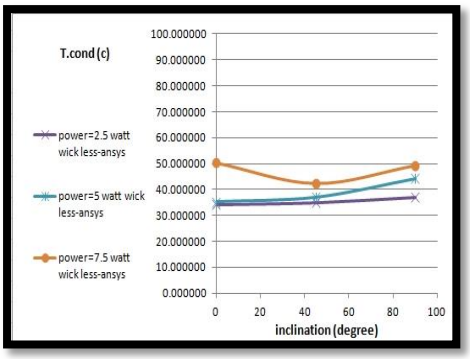

Figure (21) Condensation temperature with inclination angle for wickless heat pipe , Ansys readings.

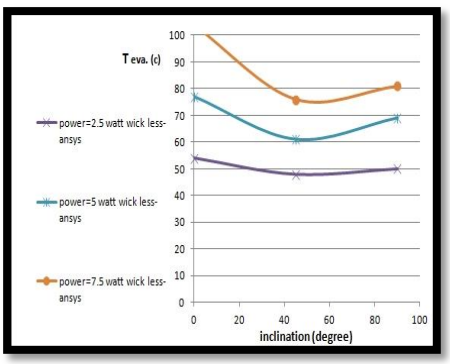

Figure (22) Evaporation temperature with inclination angle for wickless heat pipe Ansys readings

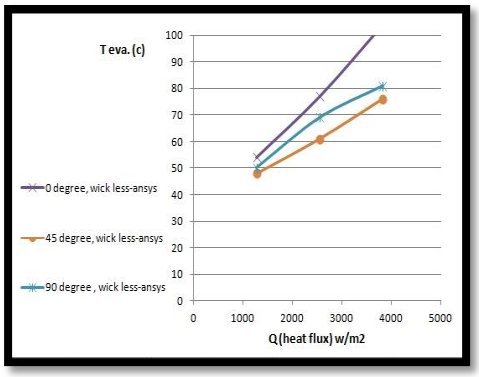

Figure (23) Evaporation temperature with thermal heat flux for wickless heat pipe , Ansys readings.

4.3 Comparison between numerical simulation and experiments results.

Based on experimental values, a simulation in ANSYS FLUENT was performed for transient operation of cooling. The main target of this simulation was to compare the practical part with simulation to calculate losses and approach real values and cooling perf. . To calculate these parameters, we should be determined the temp. distribution on the surfaces (heater, condenser) mainly. Figure (24) shows the variability in average condenser temp. with respect to heat flux for a given inclination angles for simulation and experiment , we notice that the difference obvious between plots for each case. Reason of that belong to existing a percentage of error between simulation and experiment values of condenser temperature. Figure (25) shows the variability in evaporator temp. with respect to heat flux input by the heater. Here the plots for each case almost identical, because it is the same heat flux and temperature at source. Figure (26) illustrates the variability in evaporator temp. with respect to inclination angle for three given powers, also the plots for each case identical, for same cause above. Figure (27) explain the variability in average condenser temp. with respect to inclination angle for a given powers, we recognize the difference in plots for each case. Reason belong to existing a percentage of error between simulation and experiment values of condenser temp. . If we notice from results that (2.5 W) plots for simulation and experimental results, will see match vales that's because of low temp. and pressure of system, operations of evap. and cond. occurs perfectly.

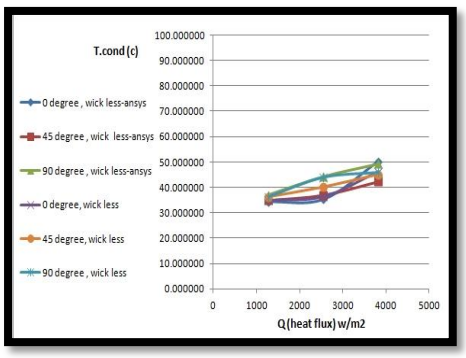

Figure (24) Condensation temperature with thermal heat flux for wickless heat pipe , Experimental & Ansys readings.

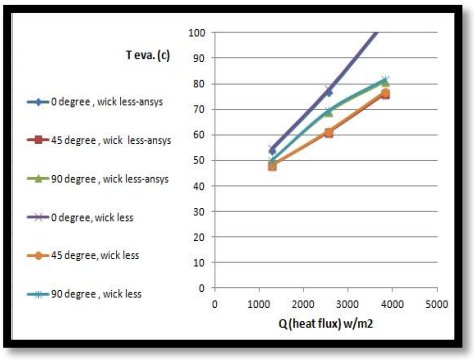

Figure (25) Evaporation temperature with thermal heat flux for wickless heat pipe , Experimental & Ansys readings

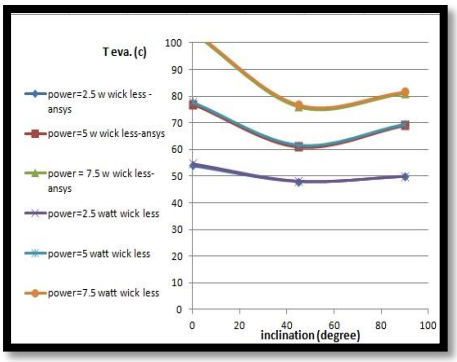

Figure (26) Evaporation temperature with inclination angle for wickless heat pipe , Experimental and Ansys readings.

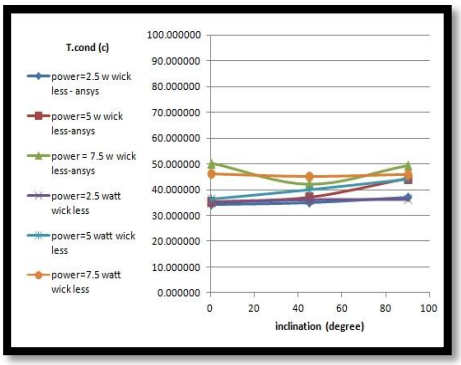

Figure (27) Condensation temperature with inclination angle for wickless heat pipe , Experimental and Ansys readings

5. Conclusion

The following points concluded from our research:

- Best inclination angle for h.p is 45°, and the thermal perf. of the h.p is optimal at this tilt angle.
- The decrement in th.r (high thermal perf.) can be noticed clearly with an increment in heat input for h.p, increasing cooling capacity.
- Thermal resistance are not effected by thermal conductivity of the h.p because of the h.t depending on the convection and vapour transmission from evaporator to condenser.
- The best behaviour of the wickless h.p be at (2.5) W through steady average temperature of condenser during (0 º , 45 º, 90 º) tilt angles.
- It observed from experimental readings, the lowest pressure at lowest temp. difference between heater and condenser sections.
- With thermal capacity increasing, pressure drop for fluid be at maximum rate, and difference in average temp. between the evaporator and condenser will increases also.
- H.p with a water as w.f is a advantage as it is readily availability and cheap in cost.
- With heat flux changing , no significant change in condenser temp.
- The findings from our research will contribute to improve current technologies, by use h.p in smart devices like (desktop computers, large printers, cleaning robots), it is reliable cooling device without noise and power consumption.

6. Recommendations for future work

- Use many types of wick h.p to study the perf. and efficiency because it's higher thermal capacity.
- Use more than one nano fluid material as working fluid to improve performance.
- Inspect many filling ratios for each working fluid chosen to reach optimum results.
- Use the self wetting system to avoid dry area in a part of heater zone, in case of (0º) inclination angle to keep steady state evaporation and condensation in system.

Nomenclature

A	Area of the heat pipe, m2
D	Diameter, m
H	Heat transfer coefficient, W/m2ºC
L	Length, m
L	Distance along the length of the heat pipe, m
R	Resistance, ºC/W
T	Thickness, m
τ	Time duration, minute
Cp	Specific heat (J kg K-1)
k	Thermal conductivity (W mK-1)
m	Mass flow rate (kg s-1)
Q	Heat input (W)
q	Heat flux (kW m-2)
CFD	Computational fluid dynamics
CSF	Continuum surface force

Dsm Mean Sauter diameter (m)
E Energy (J)
FCS Surface tension force (N)
FR Filling ratio g gravity (m/s2)
Δh Latent heat (kJ/kg)
M Molecular weight (kg/kmol)
P Pressure (Pa)
R Universal gas constant (J/mol K)
SE Energy source term (kg/m s3)
SM Momentum source term (kg/m2 s2)
T Temperature (K)
u Velocity (m/s)
UDF User-defined function
VOF Volume of fluid
WHP Wickless heat pipe
TPHP Thermal performance of heat pipe
TEHP Thermal efficiency of heat pipe
TRHP Thermal resistance of heat pipe
MCSHP Micro channel separate heat pipe
Te Temperature at Evaporator section, (C)
Tc Temperature at Condenser section, (C)
As Surface area of Evaporator section, (m2)
Q Heat input to Evaporator section, (W)
Do Outer Diameter of Heat Pipe, (m)
W.f Working fluid
Evap. Evaporation
Cond. Condensation
Th.r Thermal resistance
Temp. Temperature
Perf. Performance

Greek Symbols

Θ Inclination angle
σ $Surface\ tension\ (mN\ XV^{-1})$

References

[1] Zeina A. Abdul Redha ,A novel Design and Implementing an Annular Micro Heat Pipe Experimental System for Cooling Electronic Devices "(2017). https://doi.org/10.1109/EMS.2017.32

[2] Manimaran, R., Palaniradja, K., Alagumurthi, N., & Velmurugan, K. (2012). An investigation of thermal performance of heat pipe using Di-water. Sci Technol, 2(4), 77-80. https://doi.org/10.5923/j.scit.20120204.04

[3] Z. Xue, W. Qu, Experimental study on effect of inclination angles to ammonia pulsating heat pipe, Chinese J. Aeronaut. 27 (5) (2014) 1122–1127. https://doi.org/10.1016/j.cja.2014.08.004

[4] Senthilkumar, R., Vaidyanathan, S., & Sivaraman, B. (2012). Effect of inclination angle in heat pipe performance using copper nanofluid. Procedia Engineering, 38, 3715-3721. https://doi.org/10.1016/j.proeng.2012.06.427

[5] Fadhl, B., Wrobel, L. C., & Jouhara, H. (2013). Numerical modelling of the temperature distribution in a two-phase closed thermosyphon. Applied Thermal Engineering, 60(1-2), 122-131. https://doi.org/10.1016/j.applthermaleng.2013.06.044

[6] S.H. Noie, Heat transfer characteristics of a two-phase closed thermosiphon, Appl. Therm. Eng. 25 (4) (2005) 495–506. https://doi.org/10.1016/j.applthermaleng.2004.06.019

[7] Tang, Y., Hong, S., Wang, S., & Deng, D. (2019). Experimental study on thermal performances of ultra-thin flattened heat pipes. International Journal of Heat and Mass Transfer, 134, 884-894. https://doi.org/10.1016/j.ijheatmasstransfer.2018.12.178

[8] Zhang, H., Ye, F., Guo, H., & Yan, X. (2022). Isothermal performance of heat pipes: A review. Energies, 15(6), 1992. https://doi.org/10.3390/en15061992

[9] Maghrabie, Hussein M., et al. "Numerical simulation of heat pipes in different applications." International Journal of Thermofluids 16 (2022): 100199. https://doi.org/10.1016/j.ijft.2022.100199

[10] Tharayil, T., Asirvatham, L. G., Cassie, C. F. M., & Wongwises, S. (2017). Performance of cylindrical and flattened heat pipes at various inclinations including repeatability in anti-gravity–A comparative study. Applied Thermal Engineering, 122, 685-696. https://doi.org/10.1016/j.applthermaleng.2017.05.007

[11] M. L. Rahman, T. Afrose, H. K. Tahmina, R. P. Rinky, and M. Ali, "Effect of using acetone and distilled water on the performance of open loop pulsating heat pipe (OLPHP) with different filling ratios. 2016 .journal of applied physics. https://doi.org/10.1063/1.4958406

[12] Hu, M., Zheng, R., Pei, G., Wang, Y., Li, J., & Ji, J. (2016). Experimental study of the effect of inclination angle on the thermal performance of heat pipe photovoltaic/thermal (PV/T) systems with wickless heat pipe and wire-meshed heat pipe. Applied Thermal Engineering, 106, 651-660. https://doi.org/10.1016/j.applthermaleng.2016.06.003

[13] Q. Guo, H. Guo, X. K. Yan, F. Ye, and C. F. Ma, "Influence of inclination angle on the start-up performance of a sodium-potassium alloy heat pipe," Heat Transfer Eng., pp.(1–9, Aug. 2017). https://doi.org/10.1080/01457632.2017.1370325

[14] M.A. Chernysheva, S.I. Yushakova, Y.F. Maydanik, Copper–water loop heat pipes for energy-efficient cooling systems of supercomputers, Energy 69 (2014) 534–542. https://doi.org/10.1016/j.energy.2014.03.048

[15] Theory Guide (Release 15.0), in, ANSYS FLUENT, November 2013, pp. 475. Ansys, I. (2013). [Google Scholar]

[16] Brackbill, J. U., Kothe, D. B., & Zemach, C. (1992). A continuum method for modeling surface tension. Journal of computational physics, 100(2), 335-354. https://doi.org/10.1016/0021-9991(92)90240-Y

[17] User's Guide ANSYS Fluent (Release 15.0), Modeling Multiphase Flows, ANSYS Inc, 2015, pp. 1243–1387. [Google Scholar]

[18] J. Huang, W. Zhou, J. Xiang, C. Liu, Y.u. Gao, S. Li, W. Ling, Development of novel flexible heat pipe with multistage design inspired by structure of human spine,Appl. Therm. Eng. 175 (2020) 115392, https://doi.org/10.1016/j.applthermaleng.2020.115392

[19] A. . Abdulnabi Lazim, . A. . Daneh-Dezfuli, and L. HABEEB, "Magnetic Field Impact on Heat Transfer and Nano-Ferrofluid Flow in a Pipe", Rafidain J. Eng. Sci., vol. 2, no. 1, pp. 82–98, Dec. 2023. https://doi: 10.61268/vxe63398.

[20] A. . Hameed Hasan, S. . Mehrzad Banooni, and L. HABEEB, "Heat Transfer and Pressure Drop in Plate Fin Heat Exchangers: A Numerical Approach", Rafidain J. Eng. Sci., vol. 2, no. 1, pp. 119–135, Jan. 2024. https://doi: 10.61268/qe48kc51.

[21] bassim Al-Katib and A. . Abdullah, "Experimental and Numerical Study of the Thermal Solar Panel Performance using heated tubes: A review", Rafidain J. Eng. Sci., vol. 2, no. 1, pp. 213–224, Apr. 2024. https://doi: 10.61268/g50t3p97.